

WWOX promotes apoptosis and inhibits autophagy in paclitaxel-treated ovarian carcinoma cells

YAN ZHAO^{1,2}, WEN WANG³, WENYING PAN⁴, YUNHAI YU⁵, WENQIAN HUANG¹,
JIANGANG GAO⁶, YING ZHANG⁷ and SHIQIAN ZHANG⁸

¹School of Medicine, Shandong University, Jinan, Shandong 250012; ²Department of Gynecology and Obstetrics, Linyi People's Hospital, Linyi, Shandong 276000; ³Department of Gynecology and Obstetrics, Tengzhou Central People's Hospital, Zaozhuang, Shandong 277500; ⁴Department of Gynecology and Obstetrics, The Affiliated Hospital of Binzhou Medical College, Binzhou, Shandong 264003; ⁵Department of Gynecology and Obstetrics, The Second Hospital of Shandong University, Jinan, Shandong 250032; ⁶School of Life Sciences, Shandong University, Jinan, Shandong 250100; ⁷Department of Gynecology and Obstetrics, The First People's Hospital of Jining, Jining, Shandong 272000; ⁸Department of Gynecology and Obstetrics, Qilu Hospital, Shandong University, Jinan, Shandong 250012, P.R. China

Received May 11, 2020; Accepted November 2, 2020

DOI: 10.3892/mmr.2020.11754

Abstract. Although paclitaxel (PTX) is a first-line chemotherapeutic agent for the treatment of epithelial ovarian cancer (EOC), its clinical use is restricted by chemoresistance. Autophagy is believed to promote drug resistance, and WW domain-containing oxidoreductase (WWOX) has been predicted to serve an essential role in apoptosis induction and to suppress autophagy in various tumor cell types. In the present study, the role of WWOX was demonstrated using PTX-treated EOC cells. Cell viability and apoptosis were detected using Cell Counting Kit-8, morphological and flow cytometric analyses. WWOX and phosphorylated (p)-WWOX were highly expressed in PTX-treated sensitive EOC cells (A2780), which was accompanied by activation of the apoptosis-related proteins caspase-3 and poly (ADP-ribose) polymerase (PARP). Conversely, PTX-resistant EOC cells (A2780/T) were characterized by reduced WWOX expression and constant phosphorylation levels, as well as undetectable levels of activated caspase-3 and PARP when cells were treated with PTX. The altered expression of WWOX between the two cell types was further validated by reverse transcription-quantitative PCR. The apoptosis-inducing role of WWOX was also confirmed by flow cytometry after WWOX overexpression was induced in PTX-treated A2780 cells. These findings indicated that WWOX activation may inhibit chemoresistance and trigger cancer cell death. The upregulated expression levels

of the autophagy-related protein 12-5 complex, Beclin-1 and LC3, as well as the downregulation of P62, were also detected following PTX treatment, suggesting that PTX induced autophagic flux in both types of EOC cells. This conclusion was further supported by visualizing the accumulation of autophagosome and autolysosome vesicles, using confocal microscopy and transmission electron microscopy. PTX was also shown to inhibit mTOR signaling, indicated by a decreased level of p-mTOR and increased expression of eukaryotic translation initiation factor 4E-binding protein 1. Finally, the interaction between WWOX, mTOR and autophagy was investigated via WWOX transfection experimentation, and indicated that WWOX activated mTOR whilst inhibiting autophagy. These data indicated that WWOX may serve a critical role in PTX-induced apoptosis and could suppress autophagy by downregulating essential autophagic effectors in EOC cells via mTOR signaling.

Introduction

Epithelial ovarian cancer (EOC) is one of the most common and frequently fatal gynecological malignancies worldwide. Annually, ~230,000 women are diagnosed with EOC, resulting in 150,000 deaths (1). Since the 1980s, debulking surgery followed by chemotherapy has been the primary treatment approach for EOC, and paclitaxel (PTX) is the recommended first-line drug of choice. Although PTX treatment is initially effective, patients with advanced or relapsing tumors frequently develop chemoresistance, which further contributes to disease progression (2); however, the mechanisms underlying PTX resistance are unclear. Notably, PTX has been shown to induce autophagy in various cancer cell types, resulting in chemoresistance and a decreased rate of tumor cell death (3,4). Therefore, the discovery of novel therapeutic targets is required to overcome the autophagic effects of PTX in tumor cells.

Correspondence to: Professor Shiqian Zhang, Department of Gynecology and Obstetrics, Qilu Hospital, Shandong University, 107 Wenhua West Road, Jinan, Shandong 250012, P.R. China
E-mail: shiqianzhang370112@163.com

Key words: WWOX, ovarian cancer, autophagy, apoptosis, paclitaxel

Autophagy is an evolutionarily conserved intracellular self-defense mechanism that maintains homeostasis during a variety of stress situations, such as starvation, chemotherapy, aging-related disease and cancer (5). When autophagy is initiated, organelles and proteins are sequestered into autophagosomes that subsequently combine with lysosomes to form autolysosomes, in which cytoplasmic materials are degraded (6). Accumulating data have indicated that autophagy may be involved in the development of chemotherapeutic resistance and tumor progression in various types of cancer (7,8).

In humans, the WW domain-containing oxidoreductase (WWOX) gene is located at the ch16q23.2 or ch16q23.3-24.1 chromosomal sites, which span the common fragile site FRA16D. Due to the fragility of this genetic locus, WWOX expression is frequently lost or decreased, together with the loss of heterozygosity associated with ovarian, esophageal, breast and lung cancer (9-13). In response to stressful stimuli, WWOX is phosphorylated at Tyr33, which enables the formation of a complex containing p53 and JNK1 (14,15). Tyr33 phosphorylation and nuclear localization results in WWOX-mediated apoptosis (16). Tsai *et al* (17) revealed that WWOX may suppress autophagy and enhance methotrexate-induced death of tongue squamous cancer cells. However, studies focusing on the association between WWOX and autophagy are limited, and further analysis is required to confirm whether WWOX exerts an inhibitory effect on autophagy.

mTOR is a serine/threonine kinase, which has been reported to regulate cellular metabolism and promote proliferation in response to environmental stimuli (18). Elevated levels of mTOR phosphorylation have been predicted to be associated with diminished autophagy (18). Increasing evidence has also suggested that the relationship between mTOR signaling and autophagy is inhibitory, and that this association may act as a potential treatment target in cancer research (19,20). However, further investigation is required to confirm these findings, such as the potential mechanism of mTOR in regulating autophagy, and whether combining mTOR with WWOX may affect its downstream factors and ultimately inhibit the occurrence of autophagy.

The present study aimed to demonstrate the role of WWOX in apoptosis and autophagy during PTX treatment and to investigate the underlying mechanisms of WWOX-regulated autophagy and PTX resistance in ovarian carcinoma.

Materials and methods

Cell culture and treatment. The human EOC cell lines A2780 and SKOV3 were purchased from the American Type Culture Collection, and A2780/T cells were obtained from the Medical College of Shandong University (Jinan, China). A2780 and A2780/T cells were maintained in RPMI-1640 medium (Gibco; Thermo Fisher Scientific, Inc.) and SKOV3 cells were cultured in McCoy's 5A medium (Gibco; Thermo Fisher Scientific, Inc.). A2780/T is a PTX-resistant cell line; to maintain its drug-resistant properties, PTX (800 ng/ml) was added to the culture medium. PTX was dissolved in DMSO and then diluted with medium to the specified concentration. The SKOV3 cell line originated from the ascites of an elderly woman with moderately differentiated ovarian adenocarcinoma, which has certain tolerance to TNF and several

cytotoxic drugs. A2780 cells were derived from the ovarian tumor tissues of an untreated patient (21). PTX resistance of A2780/T cells is induced by artificial PTX treatment of A2780 cells. All of the cells were cultured at 37°C in an atmosphere containing 5% CO₂ without any antibiotics, and the media were supplemented with 10% fetal bovine serum (Moregate; Bovogen Biologicals Pty Ltd.). PTX and chloroquine (CQ) were obtained from Beijing Solarbio Science & Technology Co., Ltd. and Sigma-Aldrich (Merck KGaA), respectively. PTX and CQ were dissolved in cell medium to the specified concentration prior to use.

Cell viability detection. EOC cells were seeded (8,000 cells/well) in 96-well plates; after 24 h adhering to the plate, the cells were exposed to the indicated concentrations of PTX for 48 h in the incubator at 37°C. The treatment concentrations of PTX for A2780 and SKOV3 cells were 0.0, 3.0, 6.0, 12.5, 25.0, 50.0, 100.0 and 200.0 ng/ml. The concentrations of PTX for A2780/T cells were 0, 100, 200, 400, 800, 1,600, 2,400 and 3,200 ng/ml. Each drug concentration was repeated in five wells. Subsequently, 10 µl Cell Counting Kit-8 (Eno Gene Biotech. Co., Ltd.) solution was mixed into each well and incubated for 1 h, according to the manufacturer's protocol. A microplate reader (Thermo Fisher Scientific, Inc.) was then used to measure the optical density values at a wavelength of 450 nm. Each time point was tested in triplicate.

Western blotting. Total protein was extracted from cells using RIPA lysis buffer (Beyotime Institute of Biotechnology) and protein concentrations were quantified using a bicinchoninic acid protein kit (Pierce; Thermo Fisher Scientific, Inc.). Total proteins (30 µg) were separated by SDS-PAGE, on 15% gels for LC3 and caspase-3 detection, and 10% gels for the detection of other proteins. Proteins were transferred to PVDF membranes (EMD Millipore), which were blocked with 5% non-fat dry milk (FUJIFILM Wako Pure Chemical Corporation) or 5% bovine serum albumin (Beijing Solarbio Science & Technology Co., Ltd.) on a shaker at room temperature for 1 h, and washed in TBS-Tween (0.1% Tween-20) (Beijing Solarbio Science & Technology Co., Ltd.) for 5 sec. Then, the blots were incubated with primary antibodies at 4°C overnight. The following antibodies were used for western blot analysis: Anti-WWOX-N-terminal (cat. no. ab189410; 1:1,000; Abcam), anti-phosphorylated (p)-Y33-WWOX (cat. no. ab193624; 1:1,000; Abcam), anti-caspase-3 (cat. no. 9662; 1:1,000; Cell Signaling Technology, Inc.), anti-poly ADP-ribose polymerase (PARP; cat. no. 9542; 1:1,000; Cell Signaling Technology, Inc.), mTOR sampler kit (cat. no. 9862; 1:1,000; Cell Signaling Technology, Inc.), anti-LC3B (cat. no. 2775; 1:1,000; Cell Signaling Technology, Inc.), autophagy antibody sampler kit (cat. no. 4445; 1:1,000; Cell Signaling), anti-p62/SQSTM1 (cat. no. 18420-1-AP; 1:1,000; Proteintech Group, Inc.), anti-GAPDH (cat. no. 2605479; 1:2,000; EMD Millipore). Subsequently, membranes were washed 3 times with TBS-Tween (0.1% Tween-20) for 10 min each and incubated with a HRP-labeled secondary anti-rabbit antibody (1:1,000; cat. no. ZF-0311; OriGene Technologies, Inc.) at room temperature for 1 h. Antibody binding was visualized using ECL Plus Detection reagent (cat. no. 34080; Thermo Fisher Scientific, Inc.) and ECL film (Carestream Health,

Inc.). Images were captured using Image Lab v5.2.1 (Bio-Rad Laboratories, Inc.).

Reverse transcription-quantitative polymerase chain reaction (RT-qPCR). PBS was used to wash EOC cells twice at 4°C, and then added 1 ml TRIzol® (Invitrogen; Thermo Fisher Scientific, Inc.) was added to each well of the 6-well plate according to the manufacturer's protocol. Total RNA was obtained from cells. RT was performed using the PrimeScript RT Master Mix (Perfect Real-Time) (Takara Bio, Inc.) according to the manufacturer's instructions. qPCR was conducted using SYBR Green Master Mix (Beijing Solarbio Science & Technology Co., Ltd.) and primers designed by Wanleibio Co., Ltd. The primer sequences were as follows: WWOX, forward, 5'-GTA GAATACGCAGAACTACCAG-3' and reverse, 5'-GAACTG AGACTGTGATTGACAGAC-3'; and β -actin, forward, 5'-CTT AGTTGCGTTACACCCTTCTTG-3' and reverse, 5'-CTG TCACCTTCACCGTTCCAGTTT-3'. The reaction conditions were 95°C for 5 min, followed by 35 cycles at 95°C for 30 sec, 63°C for 30 sec and 72°C for 30 sec, and a final extension step at 72°C for 5 min. All qPCR analyses were performed in triplicate. The amplification and melting curves of the end products were obtained to confirm PCR specificity. Relative gene expression data were analyzed using RT-qPCR and the $2^{-\Delta\Delta C_q}$ method (22). Relative expression levels of genes were obtained through sequential normalization of the values against β -actin.

Flow cytometric analysis of apoptosis. EOC cells were treated with the indicated doses of PTX for 48 h in the incubator at 37°C, then harvested and resuspended in binding buffer. A2780 cells were treated with 150 ng/ml PTX; A2780/T cells were treated with 1,600 ng/ml PTX. The cells were washed twice and adjusted to a concentration of 1×10^6 cells/ml with cold D-Hanks buffer. Annexin V-Pacific Blue and propidium iodide (BioLegend, Inc.) were then added to the cell suspension and incubated for 15 min at room temperature in the dark, according to the manufacturer's instructions. Finally, 400 μ l binding buffer from the kit was added to each sample without washing, and apoptosis was analyzed using flow cytometry (BD FACSCalibur; BD Biosciences) and the data were analyzed with FlowJo software (version 7.6.1; FlowJo LLC). Each experiment was performed in triplicate.

Transfection. The eukaryotic expression vector pcDNA3.1 (cat. no. V790-20; Invitrogen; Thermo Fisher Scientific, Inc.) carrying the WWOX gene sequence (4 μ g) was transfected into A2780 and A2780/T cells (50% confluence) at room temperature and the empty pcDNA3.1 vector was used as a mock control. The WWOX mRNA fragment was synthesized by Sangon Biotech Co., Ltd. A plasmid construct containing a small interfering RNA (siRNA) targeting WWOX was generated using the mammalian expression vector pRNA-H1.1/Neo (GenScript), which was transfected into A2780 cells (50–60% confluence) with a final siRNA concentration of 100 nM at 37°C for 6 h. The WWOX-siRNA sequence was as follows: 5'-GCTGGGTTTACTACGCCAA-3'. The vector containing a scrambled sequence (GenScript) was used as a negative control (sense, 5'-TAATACGACTCACTATAG GG-3' and antisense, 5'-TAGAAGGCACAGTCGAGG-3'). The EOC cells were transfected using Lipofectamine® 2000

transfection kit (Invitrogen; Thermo Fisher Scientific, Inc.), according to the manufacturer's instructions. Following 24 h incubation at 37°C, the cells were collected for protein extraction for analysis of WWOX expression levels by western blotting as aforementioned. Monomeric red fluorescent protein (mRFP)-GFEP-LC3 adenovirus was purchased from Hanbio Biotechnology Co., Ltd. and was transfected into A2780 (MOI, 1,000) and A2780/T (MOI, 3,500) cells in 24-well dishes with 50–70% of confluence for 2 h at 37°C according to the manufacturer's protocol. The adenovirus was used to mark LC3 protein and trace autophagosome formation and degradation. After 24 h, the efficiency of adenovirus infection was confirmed by fluorescence microscopy (magnification, $\times 200$).

Confocal microscopy. A2780-mRFP-GFEP-LC3 and A2780/T-mRFP-GFEP-LC3 cells were seeded into 24-well cell culture plates at 4×10^4 cells/well. After treatment with PTX (150 ng/ml for A2780, 1,600 ng/ml for A2780/T) for 48 h at 37°C, the cells were washed with cold PBS and then fixed with 4% paraformaldehyde in PBS for 30 min at room temperature. Fixed cells were washed with PBS twice and examined under a laser scanning fluorescence confocal microscope (Leica TCS SP5; Leica Microsystems, Inc.). A total of eight images were randomly selected to determine the average number of mRFP-GFP-LC3 puncta per cell.

Transmission electron microscopy (TEM). A2780 and A2780/T cells were washed 3 times with PBS at 4°C. The adherent cells were removed and centrifuged at $1,000 \times g$ at room temperature for 10 min and fixed with 2.5% glutaraldehyde solution (Sigma-Aldrich; Merck KGaA) at 4°C for 2 h, dehydrated in a graded series of ethanol and finally embedded in resin (Ted Pella, Inc.). Ultrathin sections (70–80 nm) were prepared with an ultramicrotome (Reichert, Inc.). The thin sections were sliced and stained with 2% uranyl acetate at room temperature for 3 min, then detected using the Tecnai 10 transmission electron microscope (Philips Healthcare).

Statistical analysis. Data are presented as the mean \pm standard error of at least three experimental repeats. Comparisons with the untreated control were conducted using unpaired Student's t-test for analysis of RT-qPCR data and one-way ANOVA followed by Dunnett's multiple comparisons test for analysis of cell viability data (as shown in Fig. 1). The differences in cell viability between groups were evaluated by one-way ANOVA followed by Tukey's multiple comparisons test (as shown in Fig. S1). All statistical analyses were performed using GraphPad Prism version 8.0.2 (263) software (GraphPad Software, Inc.). $P < 0.05$ was considered to indicate a statistically significant difference.

Results

PTX inhibits cellular proliferation and induces cell death in A2780 and SKOV3 cells, but not A2780/T cells. The susceptibility of the A2780, A2780/T and SKOV3 cell lines was assessed following PTX treatment for 48 h. At 48 h, the half maximal inhibitory concentration (IC_{50}) of PTX was 167 and 371 ng/ml in A2780 and SKOV3 cells, respectively (Fig. 1A). Ultimately, a concentration of 150 ng/ml PTX was selected

for further experimentation, as it was close to the 48-h IC_{50} of A2780 cells, and is readily available. Due to their characteristic resistance to PTX, A2780/T cells were treated with a higher concentration of 1,600 ng/ml PTX, such that the observed trends were more apparent and easily interpreted. As shown in Fig. 1A and B, PTX inhibited cellular viability and induced cell death in a dose- and time-dependent manner in A2780 and SKOV3 cells, but not in A2780/T cells. Further quantification of Fig. 1B is shown in Fig. S1. In the present study, A2780/T cells proliferated well and minimal apoptosis was observed, even at the highest PTX dosage of 3,200 ng/ml. Conversely, the proliferation of A2780/T cells was accelerated with increasing drug concentrations. In addition, flow cytometric analysis revealed that PTX significantly induced cell death in A2780 cells; however, no apparent apoptosis was observed in A2780/T cells (Fig. 1C). These data clearly indicated that PTX treatment may significantly induce cell death in A2780 and SKOV3 cells, but not A2780/T cells.

Anticancer drug-induced WWOX activation reduces chemoresistance and triggers cancer cell death. There is substantial evidence to suggest that WWOX may serve a significant role in apoptosis (23,24). In the present study, the protein expression levels of WWOX were examined in three EOC cell lines and the highest protein expression levels of WWOX were observed in A2780/T cells; these cells exhibited the lowest degree of PTX sensitivity. A moderate level of WWOX expression was detected in A2780 cells and the lowest level was observed in SKOV3 cells (Fig. 2A). These observations are in contrast to those presented in previous studies, which reported the deficiency or loss of WWOX expression in more aggressive, refractory and advanced tumor cells (11,25,26). In A2780 cells, PTX upregulated the protein expression levels of WWOX in a dose- and time-dependent manner (Fig. 2C and D). In addition, the expression levels of p-WWOX (Tyr33) were increased following PTX treatment, which was accompanied by an accumulation of the cleaved forms of caspase-3 and PARP (Fig. 2D). By contrast, PTX did not increase the expression levels of WWOX or its phosphorylation in A2780/T cells (Fig. 2C and D), and the activated forms of caspase-3 and PARP were not observed at any of the post-treatment time points (Fig. 2D). The mRNA expression levels of WWOX in PTX-treated A2780 and A2780/T cells were determined using RT-qPCR analysis (Fig. 2E). PTX increased the mRNA expression levels of WWOX in A2780 cells, but downregulated its expression in A2780/T cells. Compared with in A2780 cells, a higher endogenous level of WWOX mRNA was observed in A2780/T cells. Thus, it was hypothesized that failure to induce WWOX upregulation and activation may result in chemoresistance.

WWOX was subsequently overexpressed in EOC cells using plasmid transfection (Fig. 2B). Flow cytometric analysis indicated that a higher level of WWOX expression enhanced PTX-induced apoptosis of A2780 cells (Fig. 2F). Due to ambiguously high levels of intrinsic WWOX mRNA and protein expression, and an insensitivity to PTX-induced cell death, A2780/T cells were not used for apoptosis-associated transfection experiments. In conclusion, these findings suggested that WWOX may have an important role in the induction of drug-sensitive cancer cell apoptosis.

PTX increases autophagic flux in human EOC cells. To further investigate the autophagic alterations in EOC cells, the expression levels of LC3, Beclin-1, autophagy-related protein (Atg)12-5 complex and P62 were determined. Pro-LC3 is proteolytically transformed to LC3-I, which is converted to LC3-II by ubiquitin proteases; the overall level of LC3-II indicates the extent of autophagy (27). Beclin-1 is an autophagy-specific protein that regulates autophagosome formation (28), and P62, as an autophagy-specific substrate, is incorporated into autophagosomes and consequently degraded during autophagy (29). In A2780 cells, PTX enhanced the expression levels of LC3, Beclin-1 and Atg12-5 in a time-dependent manner (Fig. 3A). Similar changes were observed in chemoresistant A2780/T cells (Fig. 3A). The expression levels of P62 were decreased in both cell lines (Fig. 3A). The endogenous levels of LC3 and Beclin-1 were higher, and the change in P62 expression occurred at an earlier stage in A2780/T cells, which implies active and persistent autophagic flux. In A2780/T cells, P62 expression was abruptly decreased after 12-h exposure to PTX. By contrast, the protein expression levels of P62 in A2780 cells were unaltered until 48 h, and was markedly decreased after 72 h (Fig. 3A). Thus, it was hypothesized that increased autophagic flux may facilitate the refractory features of A2780/T cells. Taken together, these data demonstrated that PTX could enhance the expression of multiple central autophagy-related proteins in PTX-sensitive and -resistant human EOC cells.

To monitor autophagic flux, the turnover of LC3-II protein was assessed by western blotting. Increased LC3-II levels can be interpreted as either enhanced autophagosome synthesis or reduced autophagosome turnover. In order to monitor autophagic flux induced by PTX, A2780 cells were co-treated with CQ (an autophagy inhibitor) and PTX to assess the changes in LC3-II expression, and thus, autophagic flux. LC3-II was upregulated following exposure to PTX or CQ, and was further enhanced following simultaneous treatment with both drugs, suggesting that autophagic flux was amplified by PTX, not the slow lysosomal turnover in A2780 cells (Fig. 3B).

To monitor autophagosome progression, fluorescence microscopy was used to detect GFP- and mRFP-tagged LC3-II (GFP-mRFP-LC3). Compared with those detected in untreated cells, the levels of GFP and mRFP puncta were markedly increased in A2780 cells following treatment with 150 ng/ml PTX for 48 h, indicating induced autophagic flux (Fig. 3C). By contrast, an increased number of larger sized puncta were observed in untreated A2780/T cells, which implies active basal autophagy. The number of fluorescent puncta was slightly elevated in A2780/T cells following stimulation with 1,600 ng/ml PTX for 48 h (Fig. 3C). These observations were separately validated by TEM. An increasing number of phagocytic vacuoles was also observed in the A2780 cell cytoplasm following PTX treatment (Fig. 3D). In A2780/T cells, autophagosome formation was apparent in untreated cells, and was still active following exposure to PTX (Fig. 3D). It was therefore inferred that PTX treatment may augment autophagy in EOC cells, including drug-sensitive variants.

PTX mediates the mTOR signaling pathway in EOC cells. mTOR, G β L (mLST8) and raptor comprise the mTOR complex 1 (mTORC1), which is a cellular sensor for

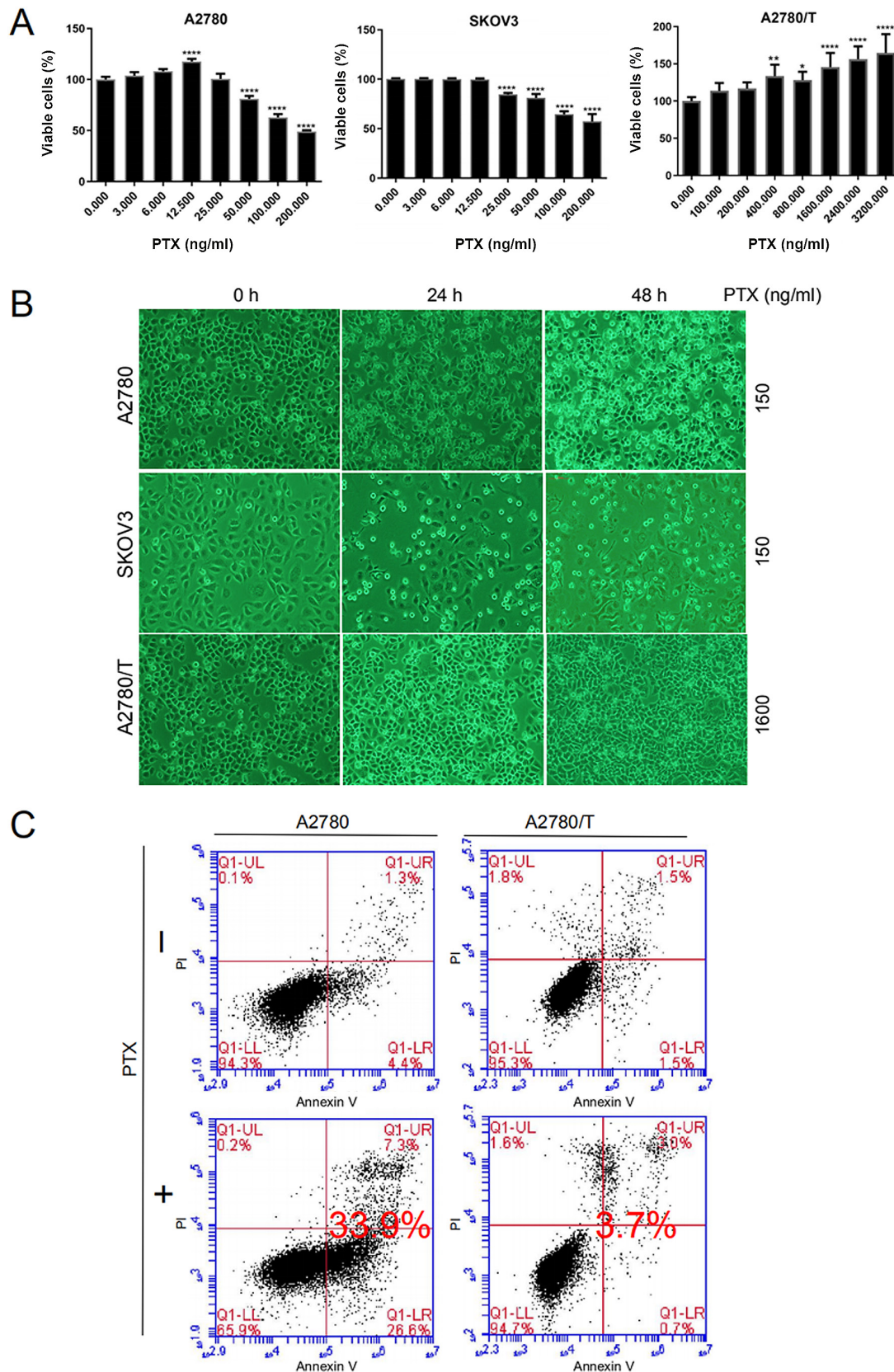


Figure 1. PTX mediates apoptotic death of EOC cells. (A) A2780, SKOV3 and A2780/T cells were seeded in 96-well plates. After 24 h, cells were treated with the indicated doses of PTX for 48 h. Cell viability was determined by Cell Counting Kit-8 assay. The percentages of viable cells were calculated vs. untreated control cells (PTX, 0 ng/ml). Representative results of three independent experiments are shown. Data are presented as the mean \pm SD. Comparisons with the untreated control group were performed by one-way ANOVA followed by Dunnett's multiple comparison test. * $P < 0.05$, ** $P < 0.01$ and **** $P < 0.0001$ vs. untreated control group. (B) A2780 and SKOV3 cells were treated with 150 ng/ml PTX for 24 and 48 h. A2780/T cells were treated with 1,600 ng/ml PTX for the indicated times. Cell morphology was observed under a light microscope (magnification, $\times 400$). Dead cells were visualized as round suspended whitish cells. (C) Annexin V and PI staining of A2780 and A2780/T cells treated with PTX for 48 h. Lower left quadrants, viable cells; lower right quadrants, necrotic cells; upper left quadrants, early apoptotic cells; upper right quadrants, nonviable late apoptotic cells. The apoptotic cell rates in A2780 and A2780/T cells were 33.9 and 3.7%, respectively. Data are representative of three independent experiments. PTX, paclitaxel; PI, propidium iodide.

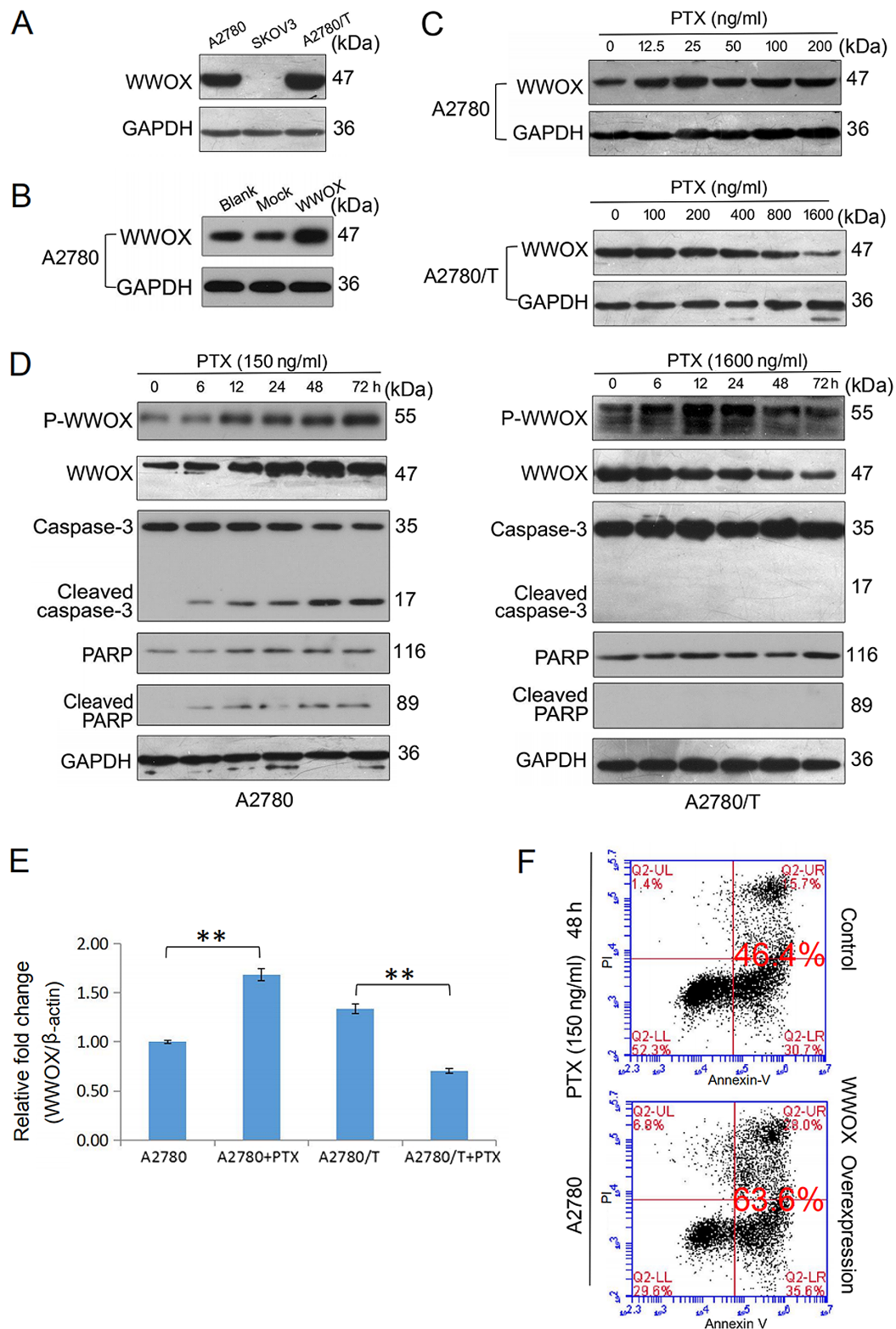


Figure 2. PTX-induced apoptotic cell death is associated with endogenous WWOX expression and activation of WWOX. (A) Western blot analysis of the protein expression levels of endogenous WWOX in A2780, SKOV3 and A2780/T cells. (B) A2780 cells were transfected with a control vector and a vector encoding human WWOX. After incubating at 37°C for 24 h, total lysates of A2780 (blank control) and transfected cells were examined for expression of WWOX by western blotting using an anti-WWOX antibody. GAPDH was used as a loading control. (C) A2780 and A2780/T cells were treated with the indicated doses of PTX for 48 h, the protein expression levels of WWOX were detected using western blotting. GAPDH was used as the internal control. (D) A2780 and A2780/T cells were treated with 150 and 1,600 ng/ml PTX, respectively. The expression levels of p-WWOX, WWOX, cleaved-caspase-3 and cleaved-PARP were determined by western blotting. GAPDH was used as the loading control. (E) A2780 and A2780/T cells were treated with 150 and 1,600 ng/ml PTX for 48 h, respectively. Quantification of WWOX mRNA expression in PTX-treated epithelial ovarian cancer cells was performed by reverse transcription-quantitative PCR analysis, and data were analyzed using the $2^{-\Delta\Delta C_t}$ method. Data are presented as the mean \pm SD. Comparisons with the untreated control were made by unpaired Student's t-test. ** $P < 0.01$. (F) A2780 cells were transfected with a vector encoding WWOX and cultured at 37°C for 24 h. Cell apoptosis was detected using Annexin V and PI staining in A2780 and transfected cells via flow cytometry. Control and WWOX overexpression cells were treated with PTX for 48 h. The apoptotic rate is indicated. Data are representative of three independent experiments. PTX, paclitaxel; WW domain-containing oxidoreductase; p-WWOX, phosphorylated-WWOX; PARP, poly (ADP-ribose) polymerase.

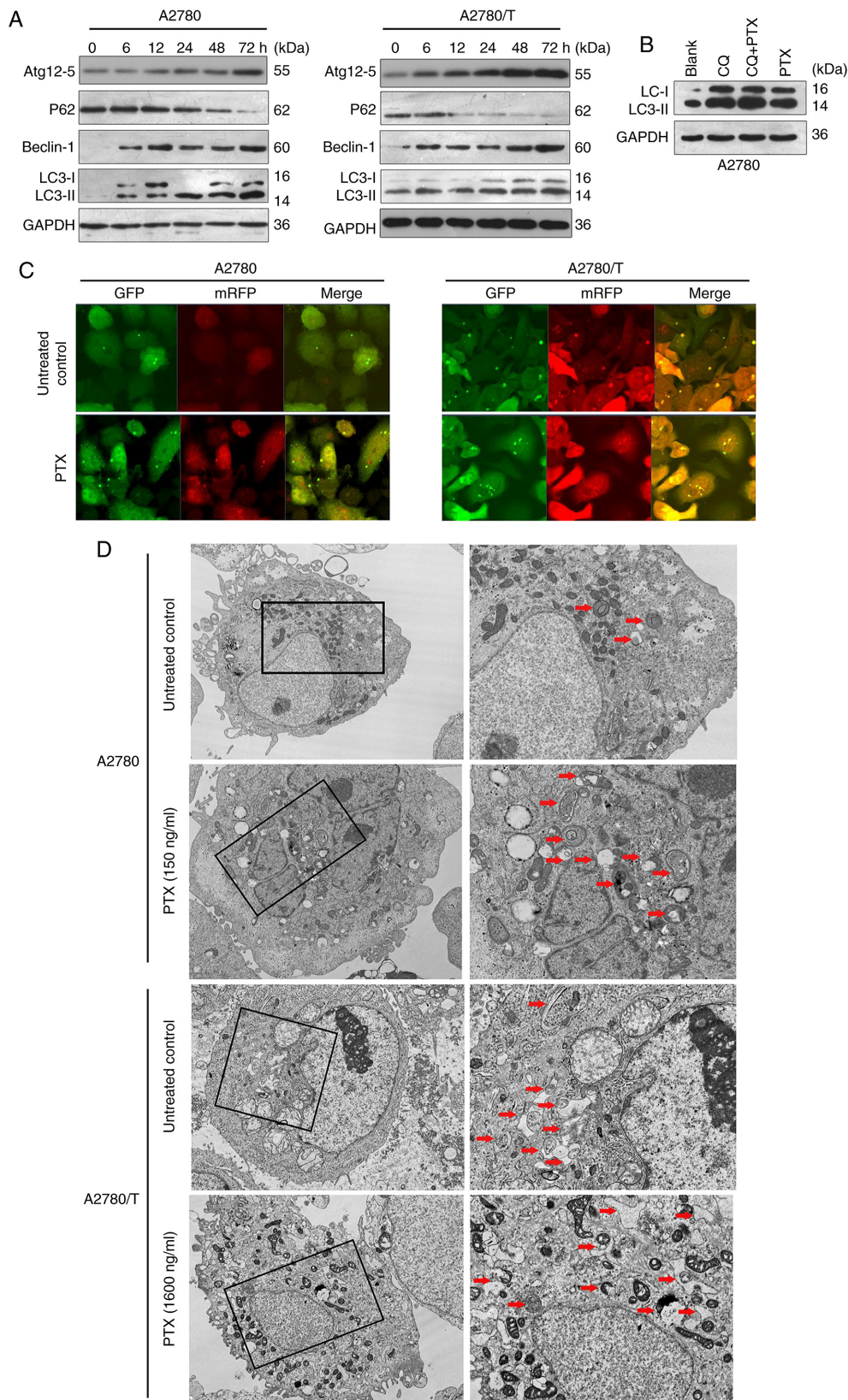


Figure 3. PTX enhances autophagy in epithelial ovarian cancer cells. (A) Total cell lysates were prepared from A2780 and A2780/T cells following treatment with 150 and 1,600 ng/ml PTX for indicated durations, respectively. The expression levels of Atg12-5, p62, Beclin-1 and LC3 were examined using western blotting. GAPDH was used as an internal control. (B) A2780 cells were treated with or without 150 ng/ml PTX in the presence or absence of CQ (25 μ M). After culturing for 24 h, cytosolic protein extracts were analyzed for LC3 protein expression. (C) A2780 and A2780/T cells were transiently transfected with GFP-mRFP-LC3 adenovirus overnight and were analyzed. After 48-h exposure to the indicated dosage of PTX (A2780, 150 ng/ml; A2780/T, 1,600 ng/ml), representative images of GFP- and mRFP-positive LC3 puncta were captured with a confocal fluorescence microscope. Cells without PTX treatment were assigned as the control. Scale bar, 20 μ m. (D) A2780 and A2780/T cells were treated with PTX for 48 h. Autophagosome and autolysosome vesicles were visualized by transmission electron microscopy. Left, magnification, $\times 10,000$; scale bar, 1 μ m. Right, magnification, $\times 30,000$; scale bar, 2 μ m. Cells without PTX treatment were assigned as the control. The typical images of autophagosomes and autolysosomes at high magnification are indicated with red arrows. PTX, paclitaxel; CQ, chloroquine; Atg12-5, autophagy-related protein 12-5 complex.

nutritional conditions that has been confirmed to negatively regulate autophagy (30). Therefore, mTOR/p70S6K signaling [mTORC1 and its downstream substrates, p-p70S6K and p-eukaryotic translation initiation factor 4E-binding protein 1 (4E-BP-1)] has been researched extensively in tumor-related studies (17,31). In the present study, the expression levels of mTOR and p-mTOR were detected, along with the downstream factors p-p70S6K kinase (Thr389 and Ser371) and p-4E-BP-1 (Thr37/46). The alterations in these target proteins during mTOR signaling were observed to be similar in PTX-sensitive and -resistant EOC cells (Fig. 4A). Furthermore, PTX suppressed the expression of p-mTOR and increased the expression levels of p-4E-BP-1 (Thr37/46). p-p70S6K kinase (at Thr389 and Ser371) was barely detected (Fig. 4A). Furthermore, to identify the potential effects of WWOX on autophagy in EOC cells, siRNA knockdown of WWOX was conducted in A2780 cells (Fig. 4B), and ectopic overexpression of WWOX was performed in A2780 and PTX-resistant A2780/T cells (Fig. 2B and 4B). The expression levels of p-mTOR in A2780 cells were decreased following siRNA-mediated WWOX-knockdown (Fig. 4C). Moreover, ectopic overexpression of WWOX increased the expression levels of p-mTOR (Fig. 4D). Thus, it was hypothesized that WWOX may interact with mTOR to mediate mTOR signaling, thus influencing its downstream targets.

WWOX inhibits autophagy in EOC cells. To ascertain the association between WWOX and autophagy, EOC cells were transiently transfected with WWOX cDNA, and the expression levels of Beclin-1 and LC3 were assessed by western blotting. Since high levels of WWOX did not promote apoptosis and activate mTOR, it was unclear whether WWOX was inactivated in A2780/T cells, thus WWOX-knockdown was conducted in A2780 cells by siRNA transfection. Upregulating WWOX expression inhibited autophagy, as evidenced by the notable reduction in Beclin-1 and LC3 in both cell lines (Fig. 4E). Conversely, the expression levels of Beclin-1 and LC3 were increased in A2780 cells following WWOX-knockdown, and further upregulated to a moderate degree following PTX administration (Fig. 4F). These findings clearly demonstrated that WWOX may suppress autophagy in human EOC cells.

Discussion

The investigation of pivotal molecules involved in drug sensitivity is an essential approach to treating cancer and targeting drug resistance; however, the related key molecules and associated mechanisms in EOC remain to be elucidated. Previous studies on WWOX have revealed some of the causes of tumorigenesis and highlighted potential methods to reverse drug resistance (16,32). WWOX is a proapoptotic protein that is believed to be tumor suppressive (33,34). In response to various stimuli, such as chemotherapeutic drug treatment and TNF, the synthesis of cytosolic WWOX has been reported to be increased and apoptosis has been shown to be induced (24). WWOX may also act as a tumor suppressor in numerous human cancer cell lines, following regulation of cancer cell biological behaviors (35). Notably, the aberrant expression of WWOX (either altered or lost) has been reported to be apparent in numerous tumor types, and may influence loss

of heterozygosity (36), gene deletion, loss of protein expression (13) and epigenetic mechanisms (10). Ectopic restoration of the WWOX gene has been shown to inhibit the growth of cervical (37), pancreatic (38) and breast cancer (39). In addition, therapeutic WWOX activation reversed temozolomide resistance and induced cancer cell death in glioblastoma (34). The results of the present study demonstrated that PTX increased WWOX expression at both the mRNA and protein levels, which was accompanied by WWOX phosphorylation and resulted in A2780 cell apoptosis. A previous study demonstrated that p-WWOX, which is generated in the cytoplasm, is primarily located in the mitochondria and translocates to the nucleus following stress stimulation, which is a requirement for WWOX-mediated apoptosis (16) p-WWOX interacts with p53, TNFR1-associated DEATH domain protein and Fas-associating death domain protein to activate caspase-8, which in turn activates caspase-9, caspase-3 and downstream PARP, ultimately resulting in cell death (16). By contrast, reduced levels of WWOX and unaltered levels of p-WWOX were detected in PTX-resistant (A2780/T) cells treated with PTX. It was hypothesized that autophagy was responsible for the accelerated A2780/T cell proliferation observed with increasing doses of PTX. Furthermore, due to its ability to support cellular metabolism via diverse nutrient sources, autophagy has been implied to promote the growth of certain tumor types (40). In the present study, an increased rate of apoptosis was observed in A2780 cells transfected with WWOX cDNA, which further verified the role of WWOX in apoptosis. These results suggested that the activation of WWOX by anticancer drugs may be essential for overcoming chemoresistance and promoting cancer cell death (6,24).

Notably, the results of the present study revealed that WWOX was substantially expressed in drug-resistant cells (A2780/T), moderately expressed in A2780 cells and largely unexpressed in SKOV3 cells; the mechanism underlying differences in WWOX expression levels in the cells is unclear. The present study was unable to explain this phenomenon (Fig. 4G), and the mechanisms associated with the high levels of WWOX and p-WWOX in resistant cells remain undetermined. However, this expression appears to be redundant, as high levels of WWOX did not effectively promote mTORC1 to inhibit autophagy in PTX-resistant cells. In addition, activated WWOX (p-WWOX) failed to elicit tumor cell death. This phenomenon cannot be explained from existing literature or the results of the present study, and the only conceivable, though somewhat implausible explanation, is the difference in cellular morphology. Taking cell line features into consideration, SKOV3 cells are morphologically more similar to interstitial cells, which may indicate a role for WWOX in epithelial-mesenchymal transition. Increased expression of WWOX may promote the retention of A2780/T cells in a normal ovarian epithelial phenotype. It has been observed that WWOX-p53 Δ oxs1 double knockout mice develop poorly differentiated osteosarcomas (14). However, differences between the expression levels of WWOX between A2780 and A2780/T cells cannot currently be explained. In resistant A2780/T cells, it was hypothesized that certain unidentified factors may cause p-WWOX to lose its apoptosis-inducing ability, and when exposed to PTX, nuclear WWOX synthesis is inhibited (Fig. 4G).

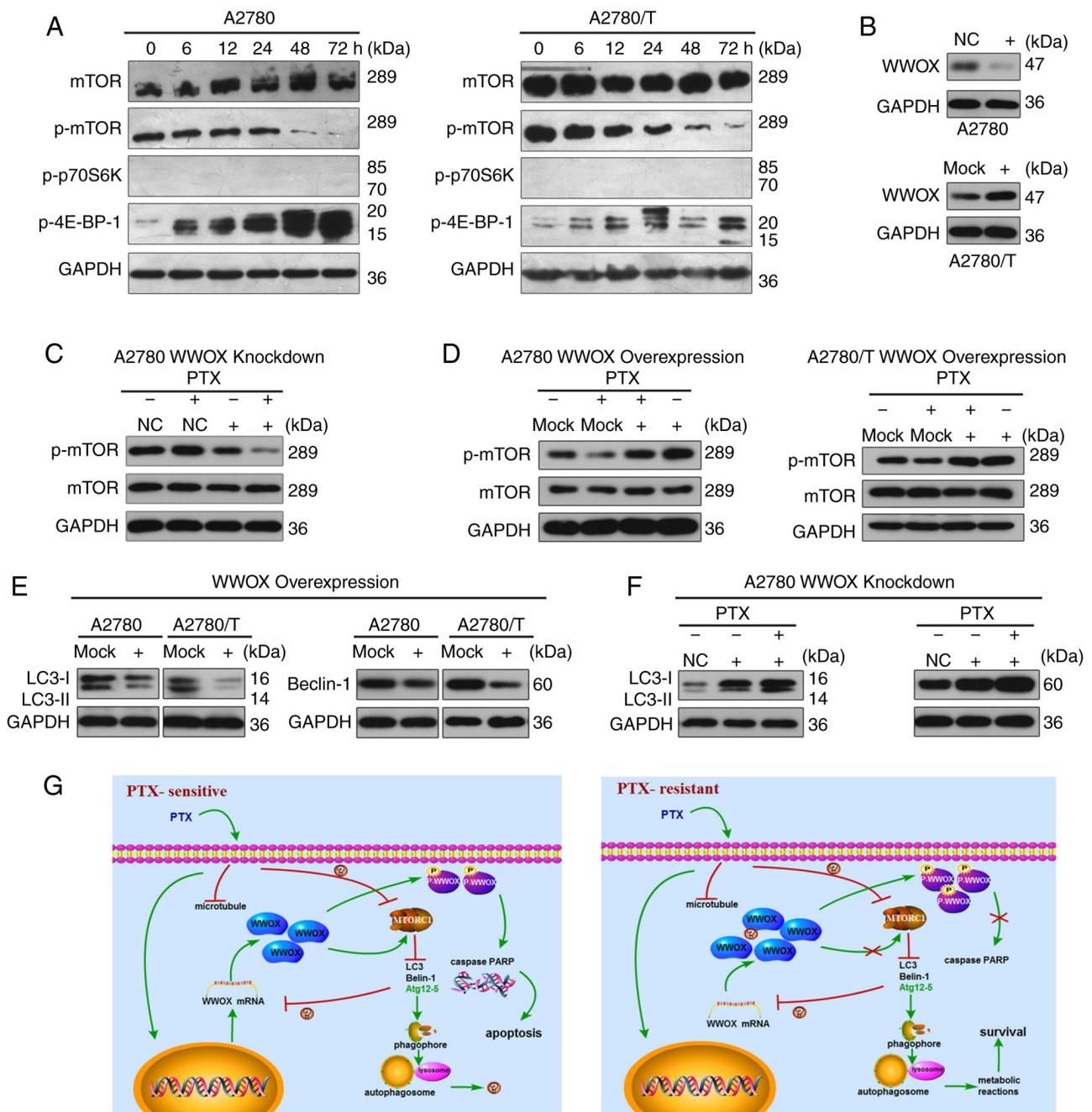


Figure 4. WWOX mediates the inhibitory effects of PTX on mTOR signaling and suppresses autophagy in epithelial ovarian cancer cells. (A) PTX reduced the expression levels of p-mTOR and increased the expression levels of p-4E-BP-1 in A2780 and A2780/T cells. Total protein extracts were prepared and analyzed using western blotting. GAPDH was used as the loading control. (B) A2780 cells were transfected with a siRNA construct targeting WWOX or a control scrambled control. A2780/T cells were transfected with a vector encoding WWOX or a control vector. (C) A2780 cells were transfected with WWOX siRNA or a control scrambled sequence; after 24 h, cells were treated with or without 150 ng/ml PTX. After culturing for 48 h, total cell lysates were detected for phosphorylation of mTOR by western blotting. GAPDH was used as the loading control. (D) A2780 and A2780/T cells were transfected with a vector encoding WWOX or a control vector and treated with 150 or 1,600 ng/ml PTX after 24 h, respectively, for 48 h. Total cell lysates were detected for phosphorylation of mTOR by western blotting. GAPDH was used as the loading control. (E) A2780 and A2780/T cells were transfected with a vector encoding WWOX or a control vector. After incubating at 37°C for 24 h, cells were cultured for another 24 h, and total cell lysates were examined for LC3 and Beclin-1 protein using western blotting. GAPDH was used as a loading control. (F) A2780 cells were infected with WWOX siRNA or a control scrambled sequence, 24 h later cells were treated with or without 150 ng/ml PTX. After culturing for 48 h, total cell lysates were detected for protein LC3 and Beclin-1. (G) Diagrams explaining the potential effects of WWOX on PTX. Left, PTX induced the upregulated level of WWOX, the phosphorylation of WWOX and increased autophagy in PTX-sensitive cells, thus resulting in apoptosis. Right, in PTX-resistant cells, PTX failed to increase the expression of WWOX and the phosphorylation of WWOX, but enhanced autophagy, resulting in cancer cell survival. PTX, paclitaxel; WW domain-containing oxidoreductase; p-, phosphorylated; siRNA, small interfering RNA; NC, negative control.

The present study did not observe apoptosis in A2780/T cells when treated with 3,200 ng/ml PTX and apoptosis induction experiments with higher concentrations of PTX were not

performed. DMSO was used to prepare stock solutions of PTX. Due to its cytotoxicity, the dosage of DMSO should be as low as possible; therefore, the concentration of PTX could

not be further increased. In addition, it was hypothesized that resistance of A2780/T cells may be enhanced due to prolonged PTX exposure.

As a potent microtubule-targeting agent, PTX is the recommended first-line chemotherapeutic drug against EOC. However, the complex mechanisms underlying PTX resistance have not yet been clarified. Cytoprotective autophagy serves an important role in chemoresistance in various types of cancer cells (41). In the present study, a higher level of intrinsic autophagy was detected in A2780/T cells compared with in A2780 cells. Thus the acquired resistance to PTX may be attributed to the robust autophagy of A2780/T cells. However, PTX induced autophagy in both susceptible and resistant EOC cells. A previous study suggested that thioredoxin domain containing 17-induced autophagy may result in PTX resistance in ovarian cancer via Beclin-1 (42). Therefore, it was hypothesized that PTX-mediated autophagy may protect EOC cells against induced apoptosis and thus promote PTX resistance.

Autophagic modulation has become increasingly important for effectively treating tumors. In numerous types of cancer, inhibiting autophagy has been shown to attenuate cellular viability and increase apoptosis (43,44). The results of the present study demonstrated that WWOX suppressed autophagy by downregulating the expression of LC3-II and Beclin-1. Furthermore, WWOX activated mTOR/p70S6K signaling and prevented the inhibitory effects of PTX. Hence, WWOX was speculated to negatively regulate autophagy by activating the mTOR signaling cascade and potentially modulating mTORC1. In view of the regulatory role of the phosphorylated proteins, western blotting was only performed for the downstream factors of mTOR (p-mTOR), p-P70S6K and p-4E-BP-1; total protein expression levels were not detected. A previous study confirmed the interaction between WWOX and mTOR (17); however, little is currently known of the exact mechanisms involved. Furthermore, the potential effects of WWOX on late-stage autophagy (i.e., the coalescence of autophagic vacuoles and liposomes) remain to be elucidated.

To the best of our knowledge, the present study is the first to indicate that in PTX-sensitive EOC cells, PTX may concurrently induce suppression of mTOR signaling and upregulation of WWOX. WWOX was demonstrated to activate mTORC1, and thus inhibit the autophagic process. From this point of view, PTX was determined to modulate autophagy by inhibiting mTORC1 in a WWOX-independent manner (Fig. 4G). Certain PTX-induced cytoplasmic factors may competitively inhibit the binding of WWOX to mTORC1. Furthermore, as PTX decreased the expression of WWOX in A2780/T cells, active autophagy may also negatively regulate WWOX (Fig. 4G).

As the mechanisms underlying the high levels of WWOX expression in drug-resistant cells are currently unknown, the existence of factors that antagonize its function cannot currently be determined. Therefore, WWOX-knockdown and the related experimental studies were not conducted in A2780/T cells in the present study. As such, the significance of WWOX in drug-resistant EOC cells requires further investigation in follow-up studies.

In conclusion, WWOX may be critical for the PTX-induced apoptosis of EOC cells, and could suppress autophagy by

downregulating essential autophagic effectors via mTOR signaling (Fig. 4G). Thus, to a certain extent, robust basal autophagy may promote PTX-resistance in A2780/T cells (Fig. 4G).

Acknowledgements

The authors would like to acknowledge the support and valuable guidance of Dr Jiangang Gao (Laboratory of Department of Life Sciences, Shandong University Central Campus).

Funding

No funding was received.

Availability of data and materials

The datasets used and/or analyzed during the current study are available from the corresponding author on reasonable request.

Authors' contributions

SZ and YZ conceived and designed the study. YZ, WW, WP, WH, YZ, YY and JG performed the experiments. YZ and SZ analyzed the data. SZ and YZ organized and wrote the manuscript. All authors read and approved the final manuscript.

Ethics approval and consent to participate

Not applicable.

Patient consent for publication

Not applicable.

Competing interests

The authors declare that they have no competing interests.

References

1. Ferlay J, Soerjomataram I, Dikshit R, Eser S, Mathers C, Rebelo M, Parkin DM, Forman D and Bray F: Cancer incidence and mortality worldwide: Sources, methods and major patterns in GLOBOCAN 2012. *Int J Cancer* 136: E359-E386, 2015.
2. Mozzetti S, Ferlini C, Concolino P, Filippetti F, Raspaglio G, Prislei S, Gallo D, Martinelli E, Ranelletti FO, Ferrandina G, *et al*: Class III beta-tubulin overexpression is a prominent mechanism of paclitaxel resistance in ovarian cancer patients. *Clin Cancer Res* 11: 298-305, 2005.
3. Veldhoen RA, Banman SL, Hemmerling DR, Odsen R, Simmen T, Simmonds AJ, Underhill DA and Goping IS: The chemotherapeutic agent paclitaxel inhibits autophagy through two distinct mechanisms that regulate apoptosis. *Oncogene* 32: 736-746, 2013.
4. Lee Y, Na J, Lee MS, Cha EY, Sul JY, Park JB and Lee JS: Combination of pristimerin and paclitaxel additively induces autophagy in human breast cancer cells via ERK1/2 regulation. *Mol Med Rep* 18: 4281-4288, 2018.
5. Zhan L, Zhang Y, Wang W, Song E, Fan Y, Li J and Wei B: Autophagy as an emerging therapy target for ovarian carcinoma. *Oncotarget* 7: 83476-83487, 2016.
6. Hale AN, Ledbetter DJ, Gawriluk TR and Rucker EB III: Autophagy: Regulation and role in development. *Autophagy* 9: 951-972, 2013.

7. Wang C, Yang Y, Sun L, Wang J, Jiang Z, Li Y, Liu D, Sun H and Pan Z: Baicalin reverses radioresistance in nasopharyngeal carcinoma by downregulating autophagy. *Cancer Cell Int* 20: 35, 2020.
8. Tyutyunyk-Massey L and Gewirtz DA: Roles of autophagy in breast cancer treatment: Target, bystander or benefactor. *Semin Cancer Biol* 66: 155-162, 2020.
9. Gao K, Yin J and Dong J: Deregulated WWOX is involved in a negative feedback loop with microRNA-214-3p in osteosarcoma. *Int J Mol Med* 38: 1850-1856, 2016.
10. Yan H, Yu N and Tong J: Effects of 5-Aza-2'-deoxycytidine on the methylation state and function of the WWOX gene in the HO-8910 ovarian cancer cell line. *Oncol Lett* 6: 845-849, 2013.
11. Guo W, Wang G, Dong Y, Guo Y, Kuang G and Dong Z: Decreased expression of WWOX in the development of esophageal squamous cell carcinoma. *Mol Carcinog* 52: 265-274, 2013.
12. Li J, Liu J, Ren Y and Liu P: Roles of the WWOX in pathogenesis and endocrine therapy of breast cancer. *Exp Biol Med* (Maywood) 240: 324-328, 2015.
13. Baykara O, Demirkaya A, Kaynak K, Tanju S, Toker A and Buyru N: WWOX gene may contribute to progression of non-small-cell lung cancer (NSCLC). *Tumour Biol* 31: 315-320, 2010.
14. Del MS, Husanie H, Iancu O, Abu-Odeh M, Evangelou K, Lovat F, Volinia S, Gordon J, Amir G, Stein J, *et al*: WWOX and p53 dysregulation synergize to drive the development of osteosarcoma. *Cancer Res* 76: 6107-6117, 2016.
15. Aderca I, Moser CD, Veerasamy M, Bani-Hani AH, Bonilla-Guerrero R, Ahmed K, Shire A, Cazanave SC, Montoya DP, Mettler TA, *et al*: The JNK inhibitor SP600129 enhances apoptosis of HCC cells induced by the tumor suppressor WWOX. *J Hepatol* 49: 373-383, 2008.
16. Chang NS, Doherty J, Ensign A, Lewis J, Heath J, Schultz L, Chen ST and Oppermann U: Molecular mechanisms underlying WOX1 activation during apoptotic and stress responses. *Biochem Pharmacol* 66: 1347-1354, 2003.
17. Tsai CW, Lai FJ, Sheu HM, Lin YS, Chang TH, Jan MS, Chen SM, Hsu PC, Huang TT, Huang TC, *et al*: WWOX suppresses autophagy for inducing apoptosis in methotrexate-treated human squamous cell carcinoma. *Cell Death Dis* 4: e792, 2013.
18. Kong W, Mao J, Yang Y, Yuan J, Chen J, Luo Y, Lai T and Zuo L: Mechanisms of mTOR and autophagy in human endothelial cell infected with dengue Virus-2. *Viral Immunol* 33: 61-70, 2020.
19. Jia J, Abudu YP, Claude-Taupin A, Gu Y, Kumar S, Choi SW, Peters R, Mudd MH, Allers L, Salemi M, *et al*: Galectins control MTOR and AMPK in response to lysosomal damage to induce autophagy. *Autophagy* 15: 169-171, 2019.
20. Munson MJ and Ganley IG: MTOR, PIK3C3, and autophagy: Signaling the beginning from the end. *Autophagy* 11: 2375-2376, 2015.
21. <https://www.atcc.org/products/all/HTB-77.aspx#characteristics>.
22. Livak KJ and Schmittgen TD: Analysis of relative gene expression data using Real-Time quantitative PCR and the 2(-Delta Delta C(T)) method. *Methods* 25: 402-408, 2001.
23. Hu BS, Tan JW, Zhu GH, Wang DF, Zhou X and Sun ZQ: WWOX induces apoptosis and inhibits proliferation of human hepatoma cell line SMMC-7721. *World J Gastroenterol* 18: 3020-3026, 2012.
24. Lo JY, Chou YT, Lai FJ and Hsu LJ: Regulation of cell signaling and apoptosis by tumor suppressor WWOX. *Exp Biol Med* (Maywood) 240: 383-391, 2015.
25. Ekizoglu S, Bulut P, Karaman E, Kilic E and Buyru N: Epigenetic and genetic alterations affect the WWOX gene in head and neck squamous cell carcinoma. *PLoS One* 10: e0115353, 2015.
26. Chen X, Li P, Yang Z and Mo WN: Expression of fragile histidine triad (FHIT) and WW-domain oxidoreductase gene (WWOX) in nasopharyngeal carcinoma. *Asian Pac J Cancer Prev* 14: 165-171, 2013.
27. Barth S, Glick D and Macleod KF: Autophagy: Assays and artifacts. *J Pathol* 221: 117-124, 2010.
28. Schmitz KJ, Ademi C, Bertram S, Schmid KW and Baba HA: Prognostic relevance of autophagy-related markers LC3, p62/sequestosome 1, Beclin-1 and ULK1 in colorectal cancer patients with respect to KRAS mutational status. *World J Surg Oncol* 14: 189, 2016.
29. Li RF, Chen G, Ren JG, Zhang W, Wu ZX, Liu B, Zhao Y and Zhao YF: The adaptor protein p62 is involved in RANKL-induced autophagy and osteoclastogenesis. *J Histochem Cytochem* 62: 879-888, 2014.
30. Kim YC and Guan KL: mTOR: A pharmacologic target for autophagy regulation. *J Clin Invest* 125: 25-32, 2015.
31. Noureldein MH and Eid AA: Gut microbiota and mTOR signaling: Insight on a new pathophysiological interaction. *Microb Pathog* 118: 98-104, 2018.
32. Yan H, Tong J, Lin X, Han Q and Huang H: Effect of the WWOX gene on the regulation of the cell cycle and apoptosis in human ovarian cancer stem cells. *Mol Med Rep* 12: 1783-1788, 2015.
33. Lin JT, Li HY, Chang NS, Lin CH, Chen YC and Lu PJ: WWOX suppresses prostate cancer cell progression through cyclin D1-mediated cell cycle arrest in the G1 phase. *Cell Cycle* 14: 408-416, 2015.
34. Chiang MF, Chou PY, Wang WJ, Sze CI and Chang NS: Tumor suppressor WWOX and p53 alterations and drug resistance in glioblastomas. *Front Oncol* 3: 43, 2013.
35. Pluciennik E, Nowakowska M, Galdyszyńska M, Popęda M and Bednarek AK: The influence of the WWOX gene on the regulation of biological processes during endometrial carcinogenesis. *Int J Mol Med* 37: 807-815, 2016.
36. Baryła I, Styczeń-Binkowska E and Bednarek AK: Alteration of WWOX in human cancer: A clinical view. *Exp Biol Med* (Maywood) 240: 305-314, 2015.
37. Hung PS, Chuang FJ, Chen CY, Chou CH, Tu HF and Lo SS: miR-187* enhances SiHa cervical cancer cell oncogenicity via suppression of WWOX. *Anticancer Res* 40: 1427-1436, 2020.
38. Nakayama S, Semba S, Maeda N, Aqeilan RI, Huebner K and Yokozaki H: Role of the WWOX gene, encompassing fragile region FRA16D, in suppression of pancreatic carcinoma cells. *Cancer Sci* 99: 1370-1376, 2008.
39. Khawaled S, Suh SS, Abdeen SK, Monin J, Distefano R, Nigita G, Croce CM and Aqeilan RI: WWOX inhibits metastasis of triple-negative breast cancer cells via modulation of miRNAs. *Cancer Res* 79: 1784-1798, 2019.
40. Kimmelman AC and White E: Autophagy and tumor metabolism. *Cell Metab* 25: 1037-1043, 2017.
41. O'Donovan TR, O'Sullivan GC and McKenna SL: Induction of autophagy by drug-resistant esophageal cancer cells promotes their survival and recovery following treatment with chemotherapeutics. *Autophagy* 7: 509-524, 2011.
42. Zhang SF, Wang XY, Fu ZQ, Peng QH, Zhang JY, Ye F, Fu YF, Zhou CY, Lu WG, Cheng XD and Xie X: TXNDC17 promotes paclitaxel resistance via inducing autophagy in ovarian cancer. *Autophagy* 11: 225-238, 2015.
43. Li LQ, Xie WJ, Pan D, Chen H and Zhang L: Inhibition of autophagy by bafilomycin A1 promotes chemosensitivity of gastric cancer cells. *Tumour Biol* 37: 653-659, 2016.
44. Polishchuk EV, Merolla A, Lichtmanegger J, Romano A, Indrieri A, Ilyechova EY, Concilli M, De Cegli R, Crispino R, Mariniello M, *et al*: Activation of autophagy, observed in liver tissues from patients with Wilson disease and from ATP7B-deficient animals, protects hepatocytes from copper-induced apoptosis. *Gastroenterology* 156: 1173-1189, 2019.